Article

A study of explosion and deformation processes of 155 mm diameter steel shell with confined explosive

Kunihiko Wakabayashi*, Masahide Katayama**, Takayuki Abe*, Eishi Kuroda*, Ken Okada*, Tomoharu Matsumura*, Yoshio Nakayama*, Mitsuaki Iida*, Masatake Yoshida*, and Shuzo Fujiwara*

This study was conducted to obtain fundamental data on the sympathetic detonation of steel shells with confined explosive for the safe treatment of munitions. In the study, we performed experiments on sympathetic detonation using steel shells with confined explosive and took high-speed framing photographs of the explosion and sympathetic detonation processes. The photographs obtained showed that the target steel shell for sympathetic detonation (the acceptor), which was placed 60 mm apart from the initiating steel shell (the donor) in series, was induced to explode by the effect of the explosion of the donor shell, indicating that shock waves generated by the impact of fragments of the donor shell initiated a chemical reaction or detonation in the neighboring acceptor shell. Whether or not the test shell was induced to detonate is considered to be strongly related to both the geometric configuration of each steel shell and the intensity of explosion of the initiating steel shell. Initial changes in the shape of the donor shell at the time of explosion were clearly observed, and the displacement of the outer wall of the shell increased with time. The temporal changes in displacement thus revealed the time-dependent acceleration processes of the outer wall. Assuming that the expansion velocity was constant, the estimated velocity was about 0.8 km $\cdot$ s^{-1} in the delay time range of 0 to 170μs after initiation of the donor. The measured terminal velocity of the fragments was found to be in the range of 0.7 to 1.3 km$\cdot$s^{-1} in the delay time range of 2 to 12 ms. These results showed good agreement with the numerical results calculated by AUTODYN-2D.

1. Introduction

The round-to-round propagation of detonation —sometimes called "sympathetic detonation"— is a process by which explosions spread rapidly in succession. We performed explosive tests to obtain fundamental information on the sympathetic detonation of steel shells with confined explosive for the safe treatment of munitions. In order to evaluate and characterize the phenomenon of sympathetic detonation, we investigated not only whether an acceptor steel shell placed around the donor steel shell would explode but also the processes inducing sympathetic detonation. The key objectives of the study were to observe the deformation processes of the steel shell exploding along with the propagation of the detonation wave inside it, and to elucidate the conditions inducing the explosion of the neighboring steel-shell confined explosive.

We took high-speed framing photographs to clarify the explosion and deformation processes of steel shell with confined explosive, and measured the expansion velocity and the velocity of the fragments using the photographs obtained.

Received : November 12, 2002
Accepted : March 10, 2003
*National Institute of Advanced Industrial Science and Technology
1−1−1 Higashi, Tsukuba Central 5, Tsukuba, Ibaraki 305-8565, JAPAN
TEL +81-298-61-4792
FAX +81-298-61-4783
E-Mail k-wakabayashi@aist.go.jp
**CRC Solutions Corp.
2−7−5 inamisuna, Koto-ku, Tokyo 136-8581, JAPAN
TEL +81-3-5634-5774
FAX +81-3-5634-7340
E-Mail m-kata@crc.co.jp

2. Experimental setup

Figure 1 shows the geometric configuration of the experimental setup. The explosive test shells consisted of a cylindrical steel casing approximately 630 mm in length and 155 mm in outside diameter with both a trinitrotoluene (TNT; ρ_0^{TNT} = 1575 kg$\cdot$m^{-3}, mass = 6.8 kg) explosive as the main charge and a picric acid (PA; ρ_0^{PA} = 1420 kg$\cdot$m^{-3}, mass = 0.097 kg) as the booster charge. Two steel shells with confined explosive were placed in series 60 mm apart from each other on a desk made of wood. One of the test shells

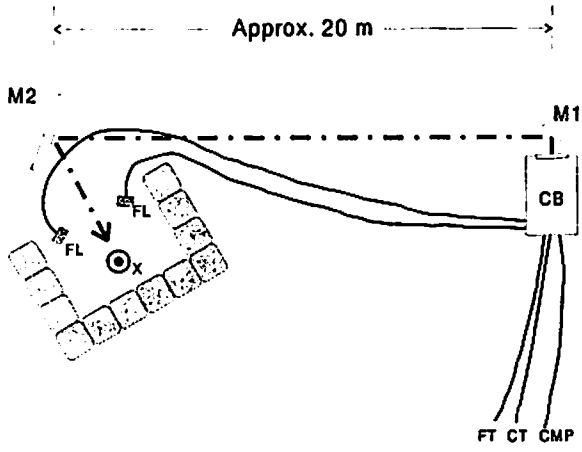

Fig.1 Schematic drawing of experimental setup for sympathetic detonation test. X: position of steel shells with confined explosives, FL: strobo-flash lighting fixture, M1: aluminum mirror (300×300 mm), M2: aluminized sheet mirror (1400×1400 mm), CB: camera box (with 2 ultrahigh-speed framing cameras (Imacon200, DRS Hadland Co. Ltd.) installed inside), FT: coaxial cable for strobo-flash trigger, CT: coaxial cable for camera trigger, CMP: coaxial cables×2 for monitor pulse from Imacon 200. Gray boxes denote bags containing sand.

(the donor) was initiated to cause a detonation by explosion of an exploding bridgewire (EBW) detonator (RP501, Reynolds Industries Inc.) via a detonating fuse (PETN, 6.5 m in length). In the experiments, two different types of cameras were used to observe the changes in shape of the steel shells resulting from the explosion. Ultrahigh-speed framing cameras (Imacon200× 2, DRS Hadland Co.) were used for the observation of ultrahigh-speed phenomena, namely, the expansion and/or deformation processes of the steel shell, expected to occur at an early stage. These two cameras allowed us to continuously record two 16-frame photographs. High-speed video cameras (Phantom V5.0× 2, recording time several seconds, Vision Research Co.) were used to observe the flight process of fragments resulting from the destruction of the steel container, over a longer time range. Both the Imacon200 and Phantom V5.0 cameras were installed in steel boxes to protect them from being damaged by the impact of fragments, and placed about 20 m and 180 m, respectively, from the point of explosion.

A number of bags containing sand were arranged around the steel shells, as shown in Fig.1. General-purpose strobo-flashes (PE-560MGN, Panasonic) were used as lighting fixtures for the steel shells. The trigger pulses (to supply power to the EBW detonator and initiate the taking of photographs) were supplied by a digital delay-pulse generator (Model 555-8ch, Berkeley Nucleonics Corp.).

3. Experimental results and discussion

Figure 2 (a) to (f) show time-resolved framing photographs obtained after initiation of the donor in the sympathetic detonation experiment using two steel shells with confined explosive. Time zero ($t_d = 0$) was the time at which the donor was initiated. The exposure time of each photograph was constant, at 1.000 ms. The white steel shell was the donor, and the black steel shell was the acceptor. The distance between the donor and the acceptor was 60 mm.

As shown in Fig.2 (a) and (b), temporal changes in the diameter of the donor steel shell, assumed to be due to the explosion effects of the explosive contained in the steel shell, were observed. The time at which the outer wall started to expand varied at different positions on the steel shell, suggesting that this phenomenon was strongly associated with the propagation of the detonation wavefront inside the shell. The photograph obtained at delay time 145μs (Fig.2 (c)) showed flames belching out from the donor. It is assumed that this was caused by cracks in the steel case wall at this stage, after which the shell broke into fragments. Furthermore, an emission was observed between the bottom of the donor and the top of the acceptor. One possibility is that the emission came from the flames belching out from cracks at the bottom of the donor case. Another possibility is that the emission was caused by the collision of fragments from the breakup of the donor with the top of the acceptor. However, it was impossible to determine the type of phenomenon that induced the emission from the experimental results alone. The photographs obtained at 281, 426, and 601μs after the explosion (Fig.2 (d), (e), and (f)) showed new flames appearing from the acceptor. The expansion process of the flames from the acceptor was similar to that from the donor, indicating that the acceptor was induced to a state of detonation or a highly reactive condition close to detonation. In this experimental condition, the experimental results indicated that a fully reactive sympathetic detonation would occur with high probability.

Knowing that the explosion of the donor induced the sympathetic detonation of the acceptor, it was necessary to elucidate the processes of the explosion of the donor shell in detail. Figure 3 shows the temporal brightness changes at the upper-side edge of the donor shell at 70, 90, 110, and 130μs after initiation. Figure 4 shows the temporal movements of the donor shell outer wall at 210 mm from the bottom edge, revealing that the displacement of the outer wall increased

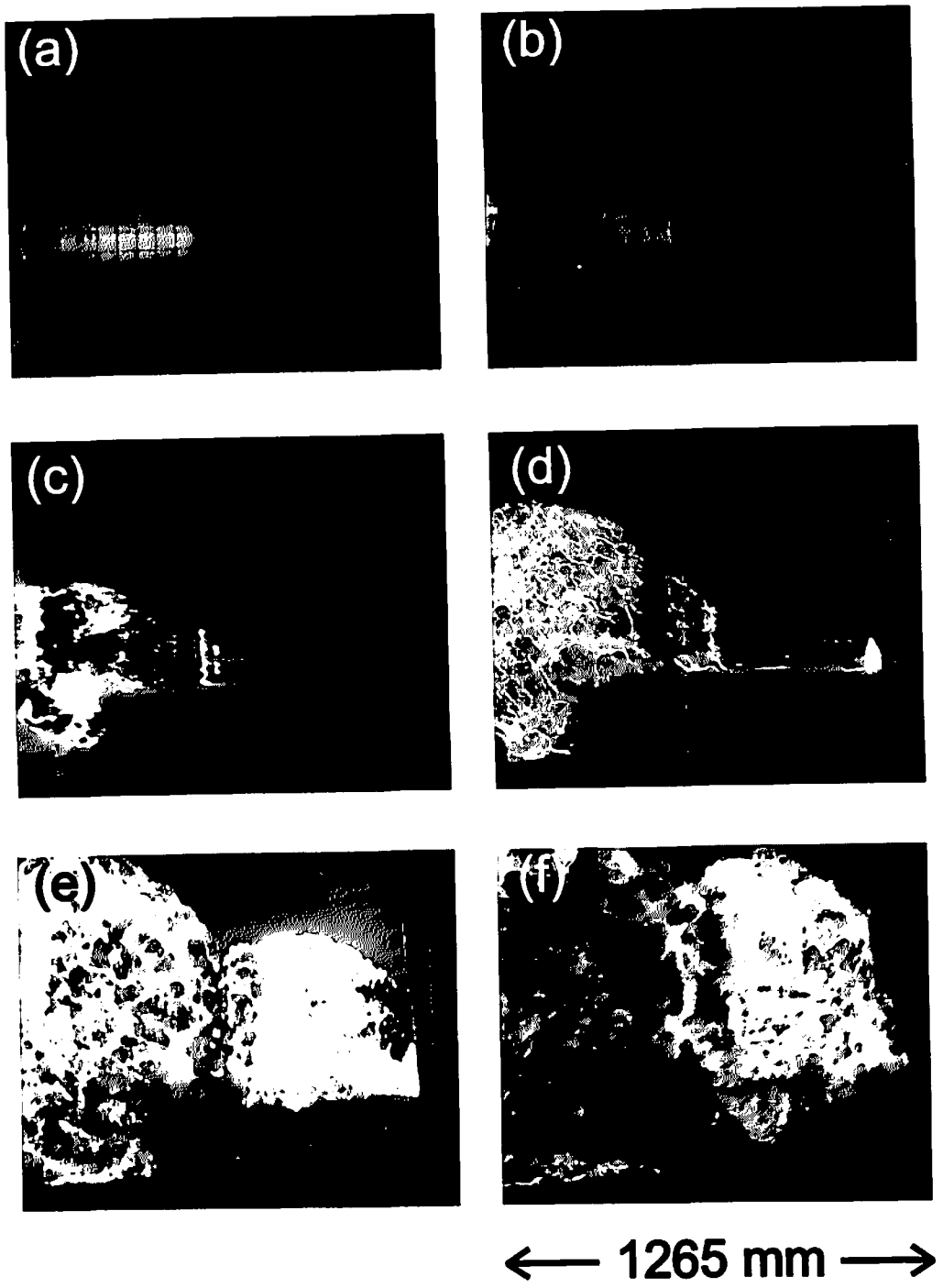

Fig.2 Time-resolved ultrahigh-speed framing photographs of sympathetic detonation experiment using two steel shells with confined explosives. The white shell was the donor, and the black shell was the acceptor. (a): 70μs, (b): 120μs, (c): 145μs, (d): 281μs, (e): 426μs, and (f): 601μs after initiation of the donor. Time zero was the initiation time of the EBW detonator attached to the donor. The exposure time was 1.000 μ s in each case.

almost linearly with the delay time. Assuming that the expansion velocity of the donor outer wall was constant, the estimated velocity was about 0.8 km · s^{-1} in the delay time range of 0 to 170μs.

Figure 5 shows a typical photograph obtained with the high-speed camera (Phantom V5.0) at 10 ms after initiation. At around this time, it can be considered that the casings of both steel shells with confined explosive (the donor and the acceptor) were completely broken into numerous fragments. Here, we paid attention to five fragments that were distinguishable to the eye as fragments generated by the explosion of the steel shells. The estimated velocity of the fragments was not constant, but was distributed in the range of 0.7 to 1.3 km · s^{-1}. These values are slightly faster than the

expansion velocity of the donor outer wall observed in the initial time region. This result leads to the interpolation that the outer wall of the steel shell accelerated with the expansion of the combustion gas of TNT, taking a few hundred microseconds to reach terminal velocity.

The maximum velocity (V_{Gurney}) of the steel shell accelerated by the detonation of the confined explosive was approximated by the Gurney formulas[1-3]. The simplest expression of the Gurney formula for a symmetrical configuration is:

$$V_{Gurney} = \sqrt{2E/(M/C + n/(n+2))}$$

where $(2E)^{1/2}$ is the Gurney constant (2316 m · s^{-1} for TNT[1]), M/C = 2.938 (M = mass of metal in the steel shell and C = mass of TNT explosive charge), and the value of n is 2 for a cylinder[4]. The upper limit of the fragment velocity was estimated to be about 1250 m · s^{-1}, and the estimated velocity was consistent with the experimental observations. However, in view of the complex mechanical and chemical processes believed to contribute to both the propagation of detonation and the deformation of the steel shell, more precise analysis using numerical simulation was required to understand this phenomenon.

4. Numerical calculation

4. 1 Hydrodynamic code

Numerical calculation was performed to elucidate the expansion and deformation processes of the steel shell after detonation of the explosive. A two-dimensional hydrodynamic code based on an explicit finite difference method, AUTODYN -2D[5], was used in this study. In this program, the material model mainly consists of two parts: (1) an equation of state describing the relationships among pressure, density, and internal energy; and (2) a material strength model for the constitutive relationships including a failure model.

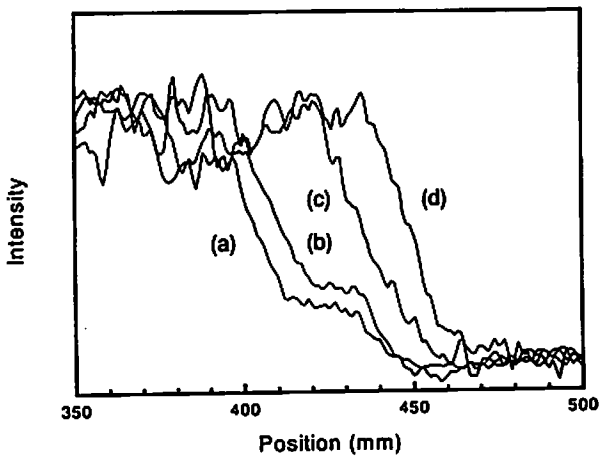

Fig.3 Brightness changes with respect to time at the upper-side edge of the donor steel-shell. (a): 70μs, (b): 90μs, (c): 110μs, and (d): 130μs after initiation of the donor.

4. 2 Modeling of 155 mm diameter cylindrical steel shell with confined explosive

The Mie-Gruneisen form of the shock Hugoniot equation of state was applied to the steel shell materials in the present study. It is known that a linear relationship between the shock

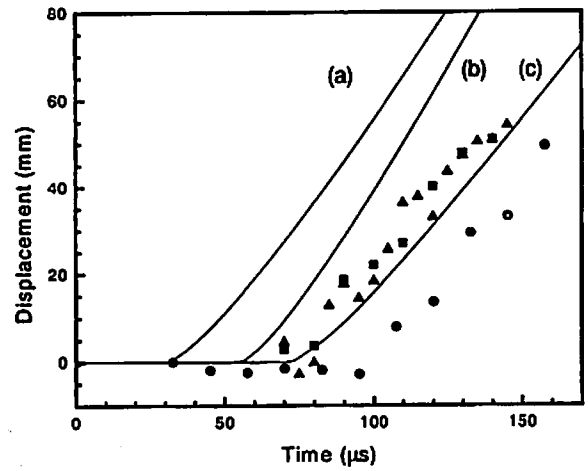

Fig.4 Changes in temporal displacement of the outer wall of the donor steel shell, including several shots. Solid symbols were experimentally obtained data at the center of the cylindrical part of the steel shell (210 mm from the bottom); ●: shot No. 1-1-1, ▲: shot No. 1-3-2, and ■: shot No. 1-3-1. The solid lines represent the numerical results at the positions of (a): 300 mm, (b): 210 mm, and (c): 90 mm from the bottom.

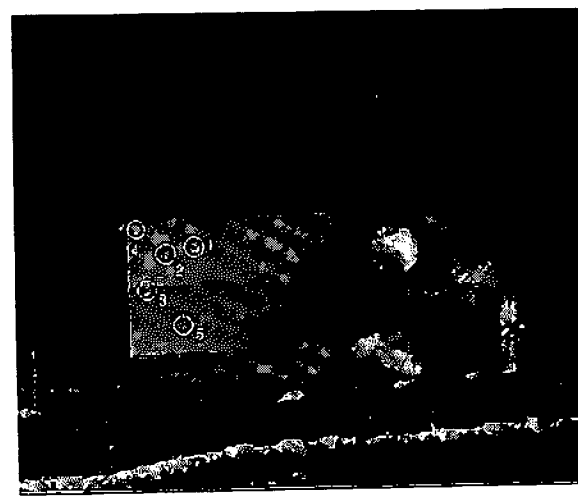

Fig.5 A typical photograph obtained with the high-speed camera (Phantom V5.0, Vision Research Co.) at 10 ms after initiation of the donor. ○ 1-5: fragments resulting from the explosion and destruction of the steel shells.

velocity and the particle velocity can adequately represent the Hugoniot for many materials that impact at a velocity less than the threshold for shock-induced vaporization.

The Steinberg-Guinan model[6] was applied as the material strength model for SCM440. The material properties of SCM440 for the Steinberg-Guinan model were not opened to the public. Therefore, the values for SS21-6-9[6] were used in place of those for SCM440, except for the density (ρ_0^{SCM440} = 7800 kg·m^{-3}), because the values of the physical properties (e.g., density, yield stress) of SS21-6-9 are almost the same as those of SCM440. Generally speaking, it can be considered that the strain-deformation is dominant in the case of high-speed deformation phenomena. In addition, the maximum effective plastic strain of materials increases with the strain rate[7]. Therefore, in the present calculation it was assumed that deformation would occur when the strain reached a value of 50%.

The JWL equation of state was applied to both of the explosives (TNT and picric acid). Material strength models for these explosives were assumed to be negligible, and the JWL EOS coefficients[8] published by the Lawrence Livermore National Laboratory were used for this calculation.

4. 3 Results of numerical calculation

In addition to the experimentally obtained results, Fig.4 also shows the simulated temporal changes of displacement of the steel shell at selected positions (300, 210, and 90 mm from the bottom). The calculated slopes of displacement with respect to time were almost linear, and agree well with the experimental results obtained at the early stage. Figure 6 shows both the time-dependent velocity changes calculated for each position and the experimental fragment velocities. It can be seen from this figure that the steel shell gradually accelerates up to the range of 0.8 to 1.3 km · s^{-1} at about 0.2 ms. Furthermore, the numerical results indicate that the terminal velocity depends on the part of the steel shell. The terminal velocity calculated by AUTODYN-2D distributed in the range of 0.8 to 1.3 km · s^{-1} coincides with the experimentally obtained results for fragment velocity (0.7 to 1.3 km · s^{-1}). Since there was no significant difference between the numerical and experimental results, the numerical model described above was judged to be reasonable, and could be useful to understand the processes of explosion of the confined explosive and deformation of the steel shell. Further research employing parametric calculations is expected to clarify the high-speed deformation processes of steel shell in more detail.

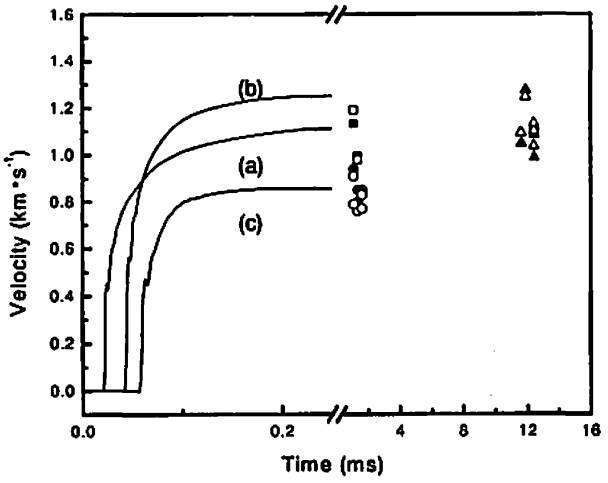

Fig.6 Temporal changes in fragment velocity. Solid lines (a), (b), and (c) indicate the numerical results at parts 300 mm, 210 mm, and 90 mm from the bottom. Symbols were experimentally obtained data at 10 ms after initiation of the donor; ●, ○: shot No. 1-1-1, ▲, △: shot No. 1-3-2, and ■, □: shot No. 1-3-1.

5. Conclusions

We performed an experiment involving the sympathetic detonation of steel shells with confined explosive, and directly observed the explosion and deformation processes by high-speed framing photography. The photographs obtained showed that the acceptor charge placed 60 mm from the donor charge in series was induced to explode. The expansion velocity of the donor shell was about 0.8 km · s^{-1} at an early stage, and the subsequent velocity of fragments was distributed in the range of 0.7 to 1.3 km · s^{-1}. Numerical calculation was also performed to elucidate the high-speed deformation processes. The calculated results showed good agreement with the experimental results.

Acknowledgments

This study has been done under the auspices of the ACW Office of the Cabinet Office and the Japan Institute of International Affairs. The authors would like to thank Mr. H. Sasaki, Mr. K. Niwa, and Mr. R. Marumo of nac Image Technology Inc., and Mr. N. Konishi, Mr. T. Yoshida, and Mr. H. Usui of Nobby Tech Ltd., for their technical support of high-speed framing photography.

References

1) A. C. Victor. Propellants, Explosives and Pyrotechnics, 21,90, 1996.

2) J. T. Dehn. "Models of Explosively Driven Metals." Eighth Symposium (International) on Detonation,

Albuquerque, New Mexico, July 15-19, 1985, NSWC MP 86-194, [Proc.], pp.602-612, 1985.

3) J. G. Glenn and M. Gunger. "Simulating Sympathetic Detonation Effects." Tenth International Detonation Symposium, Boston, Massachusetts, July 12-16, 1993, ONR 33395-12, [Proc.], pp. 928-935, 1993.

4) B. T. Fedoroff and O. E. Sheffield. Encyclopedia of Explosives and Related Items, 6, G195, 1974.

5) AUTODYN-2D User Manual, Revision 4.2. Century Dynamics, San Ramon, California, 2001.

6) D. S. Steinberg. "Equation of State and Strength Properties of Selected Materials." UCRL-MA-106439, Lawrence Livermore National Laboratory, Feb. 1991.

7) M. Katayama, S. Kibe and S. Toda. "A numerical simulation method and its validation for debris impact against the whipple bumper shield." International Journal of Impact Engineering, 17,465, 1995.

8) E. Lee, M. Finger and W. Collins. "JWL equation of state coefficients for high explosives." UCID-16189, Lawrence Livermore Laboratory, Jan. 1973.